

Lattice dynamics of Ni₃Al

C. Stassis, F. X. Kayser, C.-K. Loong, and D. Arch

*Ames Laboratory, U. S. Department of Energy, Iowa State University, Ames, Iowa 50011
and Department of Physics, Iowa State University, Ames, Iowa 50011*

(Received 2 April 1981)

The intermetallic compound Ni₃Al orders in the Cu₃Au structure, and it is generally believed to be a weak itinerant ferromagnet. However, the presence of any magnetic inhomogeneities, as suggested by specific-heat measurements, cannot be easily understood within the framework of an itinerant electron theory. In the present work inelastic neutron scattering techniques have been used to study the room-temperature phonon dispersion curves of Ni₃Al. The force constants obtained by fitting the experimental data to a three-nearest-neighbor Born-von Kármán model were used to evaluate the phonon density of states and the lattice specific heat. We find that the electronic specific heat of Ni₃Al (obtained by subtracting the lattice contribution from the measured total specific heat) does not exhibit any anomalous features at low temperature. Thus, within experimental precision, we do not find any evidence for the presence of magnetic inhomogeneities in Ni₃Al.

I. INTRODUCTION

The physical properties of the Ni_{3+x}Al_{1-x} (and Ni_{3+x}Ga_{1-x}) alloys, for compositions close to that of the Ni₃Al (and Ni₃Ga) compound, have been studied extensively.¹⁻⁹ In a relatively narrow composition range (~73.5–76 at. % Ni) the Ni_{3+x}Al_{1-x} alloys order in the Cu₃Au crystal structure and exhibit rather remarkable magnetic properties. In the 73.5–74.6 at. % composition range the alloys are paramagnetic whilst those with higher nickel content are ferromagnetic, with a ferromagnetic moment and Curie point which vary continuously with composition. This observation, the temperature dependence of the magnetization curves and the large high-field differential susceptibility of these ferromagnetic alloys all suggest¹⁻⁹ that these systems behave like weak itinerant ferromagnets. Actually band-theoretical calculations^{10,11} led to a qualitative understanding of the magnetic properties of these ferromagnetic alloys.

Quite recently, however, anomalies have been observed⁴⁻⁶ in the low-temperature specific heat of Ni₃Al as well as in a large number of nonstoichiometric Ni_{3+x}Al_{1-x} ordered alloys. The shape of these anomalies has suggested an additional contribution to the specific heat arising from the presence of magnetic inhomogeneities.⁴⁻⁷ However, such an interpretation does not provide a satisfactory explanation of the specific-heat measurements.⁶ Moreover, the presence of any magnetic inhomogeneities cannot be easily understood within the framework of an itinerant electron theory. Certainly a determination of the lattice specific heat would help in assessing the presence of any anomalous features in the electronic contribution to the total specific heat of Ni₃Al.

The elastic and lattice-dynamical properties of Ni₃Al are also of considerable technological interest. This compound is in fact considered^{12,13} as the

principal hardening phase (γ') in various nickel-based high-temperature alloys. We were thus motivated to initiate a systematic study of the elastic constants and lattice dynamics of this compound. Our ultrasonic measurements of the elastic constants of Ni₃Al were reported in an earlier communication.¹⁴ In the present paper we present the results of an inelastic neutron scattering investigation of the lattice dynamics of this compound.

II. EXPERIMENTAL DETAILS

The measurements were performed on a large (~4 cm³) single crystal of Ni₃Al prepared in the Ames Laboratory. A polycrystalline sample was first prepared by arc-melting (under a partial pressure of helium) appropriate quantities of 99.999% pure Al and 99.8% pure Ni. The nickel was found to contain 0.04% by weight sulfur as the major impurity. The crystal was grown in a pre-fired calcia-stabilized zirconia crucible, using a modified Bridgman technique. The as-grown crystal was annealed for six days in air at 1268 °C. Examination of metallographically polished and electroetched faces did not reveal any evidence of dendritic or cellular segregation. After completion of the operations involved in shaping the crystal (cutting, grinding, and lapping), the sample was heated at 905 °C for six hours and then it was slowly cooled to room temperature in steps of 50 °C/day to minimize any atomic disordering produced by cold work damage. Sections cut parallel to two of the (110) faces and one of the (001) faces during the sample preparation were chemically analyzed. The results have shown that the crystal was chemically homogeneous and of stoichiometric composition.

The phonon dispersion curves of Ni₃Al were determined using two triple-axis spectrometers, one

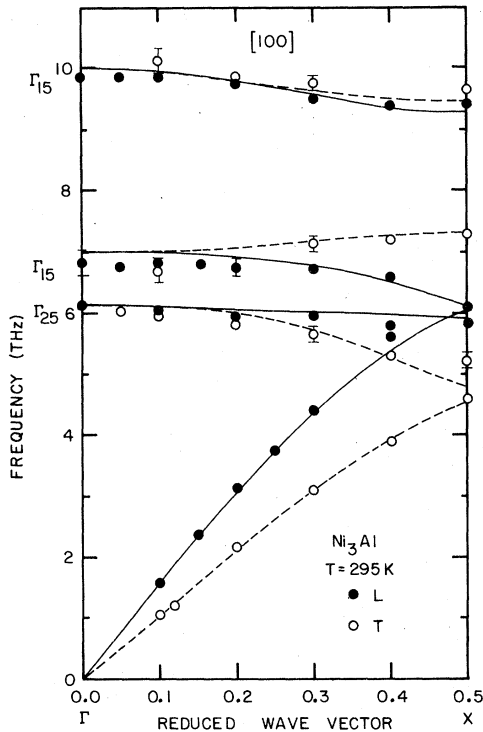


FIG. 1. Phonon dispersion curves of Ni₃Al along the [100] symmetry direction at room temperature. The solid and dashed lines are purely longitudinal (Δ_1 's and Δ_2) and purely transverse (Δ_3 's) branches, respectively, obtained by fitting the data to a three-nearest-neighbor Born-von Kármán model.

at the Oak Ridge Research Reactor (ORR) and the other at the High-Flux Isotope Reactor (HFIR) of the Oak Ridge National Laboratory. With few exceptions the data were collected with the spectrometer in the constant- \bar{Q} mode of operation (where \bar{Q} denotes the neutron scattering vector). Most data were taken using a constant scattered neutron energy of 3.6 THz and a pyrolytic graphite filter to attenuate higher-order contaminations. The following monochromator (reflecting plane) collimation before sample collimation after sample analyzer (reflecting plane) combinations were used: PG(002)-40'-40'-PG(002), PG(002)-40'-60'-PG(002), PG(004)-40'-40'-PG(002), PG(004)-40'-60'-PG(004), PG(004)-40'-40'-Ge(111), Be(002)-40'-60'-PG(002), where PG denotes pyrolytic graphite. In most measurements pyrolytic graphite reflecting from the (002) or (004) planes was used as monochromator. However, to resolve the structure of the dispersion curves, measurements with better energy resolution were necessary and in these scans Be was used as a monochromator. The measurements were performed in the (100), (1 $\bar{1}$ 0), (1 $\bar{1}$ 1), and (11 $\bar{2}$) symmetry planes, and the

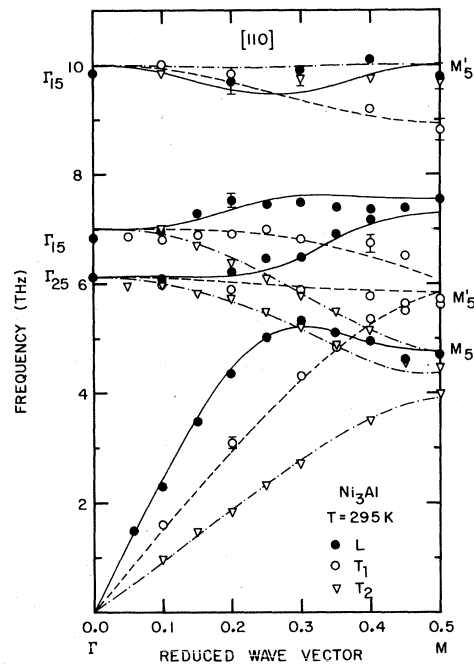


FIG. 2. Phonon dispersion curves of Ni₃Al along the [110] symmetry direction at room temperature. The solid, dashed, and point-dashed lines are longitudinal-like (Σ_1 's), purely transverse (Σ_3 's and Σ_2), and transverselike (Σ_4 's) branches, respectively, obtained by fitting the data to a three-nearest-neighbor Born-von Kármán model.

dispersion curves were identified by comparing the intensities of the measured neutron groups with calculations based on force-constant models. A large number of phonon frequencies were determined under different experimental conditions and were found to agree to within experimental precision.

III. EXPERIMENTAL RESULTS AND DISCUSSION

The room-temperature dispersion curves of Ni₃Al were determined along the [100], [110], and [111] symmetry directions. The assignment of the measured phonon frequencies to various branches adopted in presenting the data is that which provided the best agreement between the experimentally measured phonon frequencies and intensities and calculations based on a three-nearest-neighbor Born-von Kármán model. The measured phonon frequencies (assigned to various branches as we described) are listed in Table I and the room-temperature dispersion curves are plotted in Figs. 1-3.

TABLE I. Measured phonon frequencies (in THz) of Ni₃Al at room temperature, along the [100], [110], and [111] symmetry directions.

ξ	ν	ξ	ν	ξ	ν	ξ	ν
LA[$\xi 00$] Δ_1		LO ₁ [$\xi 00$] Δ_2		LO ₂ [$\xi 00$] Δ_1		LO ₃ [$\xi 00$] Δ_1	
0.1	1.57 ± 0.03	0	6.12 ± 0.15	0	6.83 ± 0.15	0	9.85 ± 0.15
0.15	2.35 ± 0.05	0.1	6.00 ± 0.13	0.05	6.75 ± 0.12	0.05	9.85 ± 0.13
0.2	3.12 ± 0.07	0.2	5.92 ± 0.12	0.1	6.80 ± 0.15	0.1	9.87 ± 0.15
0.25	3.73 ± 0.08	0.3	5.96 ± 0.12	0.15	6.81 ± 0.10	0.2	9.74 ± 0.10
0.3	4.41 ± 0.05	0.4	5.80 ± 0.10	0.2	6.74 ± 0.13	0.3	9.52 ± 0.15
0.4	5.60 ± 0.08	0.5	5.82 ± 0.11	0.3	6.72 ± 0.20	0.4	9.40 ± 0.12
0.5	6.11 ± 0.06			0.4	6.59 ± 0.15	0.5	9.45 ± 0.08
TA[$\xi 00$] Δ_5		TO ₁ [$\xi 00$] Δ_5		TO ₂ [$\xi 00$] Δ_5		TO ₃ [$\xi 00$] Δ_5	
0.1	1.14 ± 0.04	0.05	6.03 ± 0.12	0.1	6.70 ± 0.20	0.1	10.14 ± 0.20
0.12	1.20 ± 0.04	0.1	5.98 ± 0.13	0.3	7.13 ± 0.10	0.2	9.87 ± 0.15
0.2	2.16 ± 0.05	0.2	5.83 ± 0.10	0.4	7.21 ± 0.10	0.3	9.77 ± 0.15
0.3	3.08 ± 0.05	0.3	5.65 ± 0.12	0.5	7.29 ± 0.10	0.5	9.68 ± 0.15
0.4	3.88 ± 0.06	0.4	5.28 ± 0.10				
0.5	4.59 ± 0.04	0.5	5.22 ± 0.12				
LA[$\xi \xi 0$] Σ_1		LO ₁ [$\xi \xi 0$] Σ_1		LO ₂ [$\xi \xi 0$] Σ_1		LO ₃ [$\xi \xi 0$] Σ_1	
0.059	1.50 ± 0.06	0.1	6.10 ± 0.15	0.1	6.98 ± 0.12	0.2	9.70 ± 0.25
0.1	2.30 ± 0.08	0.2	6.22 ± 0.10	0.15	7.30 ± 0.10	0.3	9.90 ± 0.10
0.15	3.49 ± 0.06	0.25	6.47 ± 0.08	0.2	7.52 ± 0.08	0.4	10.10 ± 0.20
0.2	4.36 ± 0.05	0.3	6.48 ± 0.10	0.25	7.44 ± 0.10	0.5	9.80 ± 0.20
0.25	5.02 ± 0.07	0.35	6.91 ± 0.08	0.3	7.48 ± 0.10		
0.3	5.32 ± 0.05	0.4	7.18 ± 0.10	0.35	7.40 ± 0.15		
0.35	5.10 ± 0.05	0.45	7.40 ± 0.10	0.4	7.35 ± 0.15		
0.4	4.94 ± 0.07	0.5	7.55 ± 0.12				
0.45	4.62 ± 0.07						
0.5	4.70 ± 0.07						
TA[$\xi \xi 0$] Σ_3		TO ₁ [$\xi \xi 0$] Σ_2		TO ₂ [$\xi \xi 0$] Σ_3		TO ₃ [$\xi \xi 0$] Σ_3	
0.1	1.62 ± 0.06	0.1	6.00 ± 0.12	0.05	6.87 ± 0.20	0.1	10.02 ± 0.20
0.2	3.10 ± 0.08	0.2	5.90 ± 0.25	0.1	6.80 ± 0.15	0.2	9.83 ± 0.25
0.3	4.31 ± 0.06	0.3	5.87 ± 0.20	0.15	6.90 ± 0.20	0.4	9.20 ± 0.20
0.35	4.84 ± 0.06	0.4	5.79 ± 0.10	0.2	6.91 ± 0.15	0.5	8.82 ± 0.20
0.4	5.36 ± 0.06	0.45	5.65 ± 0.15	0.25	7.00 ± 0.15		
0.45	5.52 ± 0.10	0.5	5.62 ± 0.20	0.3	6.83 ± 0.12		
0.5	5.70 ± 0.15			0.4	6.74 ± 0.15		
				0.45	6.53 ± 0.12		
TA[$\xi \xi 0$] Σ_4		TO ₁ [$\xi \xi 0$] Σ_4		TO ₂ [$\xi \xi 0$] Σ_4		TO ₃ [$\xi \xi 0$] Σ_4	
0.1	1.00 ± 0.02	0.05	5.96 ± 0.15	0.1	7.02 ± 0.12	0.1	9.86 ± 0.12
0.15	1.48 ± 0.03	0.1	5.99 ± 0.15	0.15	6.70 ± 0.15	0.3	9.76 ± 0.15
0.2	1.86 ± 0.04	0.15	5.84 ± 0.10	0.2	6.40 ± 0.15	0.4	9.76 ± 0.15
0.25	2.33 ± 0.03	0.2	5.75 ± 0.12	0.25	6.11 ± 0.07	0.5	9.70 ± 0.15
0.3	2.72 ± 0.06	0.25	5.50 ± 0.10	0.3	5.82 ± 0.05		
0.4	3.51 ± 0.05	0.3	5.20 ± 0.10	0.35	5.51 ± 0.06		
0.5	3.98 ± 0.07	0.35	4.89 ± 0.15	0.4	5.16 ± 0.06		
		0.45	4.56 ± 0.20				
		0.5	4.48 ± 0.08				
LA[$\xi \xi \xi$] Λ_1		LO ₁ [$\xi \xi \xi$] Λ_3		LO ₂ [$\xi \xi \xi$] Λ_1		LO ₃ [$\xi \xi \xi$] Λ_1	
0.05	1.75 ± 0.06	0.05	6.38 ± 0.15	0.1	7.03 ± 0.12	0.1	9.60 ± 0.15
0.1	3.13 ± 0.05	0.1	6.40 ± 0.10	0.25	7.75 ± 0.15	0.2	9.06 ± 0.15
0.15	4.35 ± 0.09	0.15	6.46 ± 0.10	0.3	8.00 ± 0.18	0.3	9.50 ± 0.15
0.2	5.45 ± 0.12	0.2	6.30 ± 0.15	0.4	8.47 ± 0.25		
0.25	5.82 ± 0.15	0.25	6.10 ± 0.15	0.5	8.85 ± 0.25		
0.3	6.10 ± 0.15	0.3	5.78 ± 0.20				
0.35	5.84 ± 0.10	0.35	5.24 ± 0.15				

TABLE I. (Continued.)

ξ	ν	ξ	ν	ξ	ν	ξ	ν
0.45	5.69 ± 0.12	0.4	4.90 ± 0.20				
0.5	5.77 ± 0.20	0.45	4.30 ± 0.15				
		0.5	4.48 ± 0.22				
TA[$\xi\xi\xi$]A ₃		TO ₁ [$\xi\xi\xi$]A ₂		TO ₂ [$\xi\xi\xi$]A ₃		TO ₃ [$\xi\xi\xi$]A ₃	
0.1	1.30 ± 0.04	0.05	6.15 ± 0.20	0.1	7.15 ± 0.10	0.1	10.05 ± 0.15
0.2	2.50 ± 0.06	0.1	6.24 ± 0.25	0.15	6.75 ± 0.15	0.15	10.21 ± 0.20
0.3	3.45 ± 0.15	0.2	5.93 ± 0.20	0.25	6.50 ± 0.15	0.25	9.95 ± 0.20
0.4	4.03 ± 0.12	0.3	5.40 ± 0.20	0.3	6.60 ± 0.15	0.3	10.00 ± 0.15
0.45	4.00 ± 0.12	0.45	4.41 ± 0.20	0.35	6.45 ± 0.12	0.4	10.07 ± 0.25
0.5	4.10 ± 0.15	0.5	4.30 ± 0.25	0.45	5.95 ± 0.15	0.5	10.20 ± 0.20

Examination of Figs. 1–3 does not reveal, in general, any pronounced anomalies in the dispersion curves of Ni₃Al. In addition, we did not observe any unusual features in the temperature dependence of the elastic constants of this compound. Thus both the elastic as well as the lattice-dynamical properties of Ni₃Al do not appear to be affected

by the interaction of the lattice^{15,16} with dislocations, which are generally believed to be responsible for the sevenfold increase with increasing temperature (between approximately liquid nitrogen and 900 K) in the flow strength of this compound.

To obtain the lattice specific heat of Ni₃Al, the experimental results were analyzed using a conventional Born–von Kármán force-constant model. It can be seen (Figs. 1–3) that a three-nearest-neighbor force-constant model (18 independent force constants) provides an adequate fit to the experimentally determined dispersion curves of Ni₃Al. The force constants obtained by fitting the experimental data to this three-nearest-neighbor model are listed in Table II. The elastic constants obtained (see Table II) using this model are in good agreement with the values determined in our ultrasonic measurements.¹⁴ It is interesting to note that the first-nearest-neighbor Ni–Ni forces and the elastic constants of Ni₃Al are comparable to those of pure nickel.^{17–19}

The force constants listed in Table II were used to evaluate the phonon density of states $g(\nu)$ by the tetrahedron method.²⁰ The phonon density of states

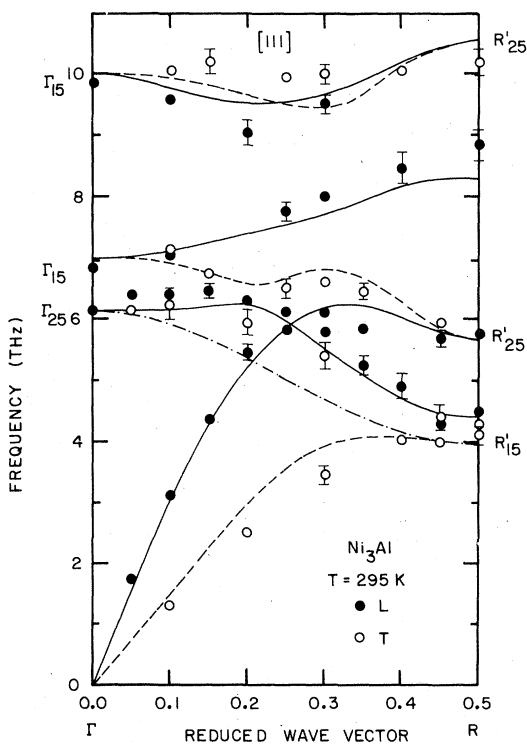


FIG. 3. Phonon dispersion curves of Ni₃Al along the [111] symmetry direction at room temperature. The solid, dashed, and point-dashed lines are longitudinal-like (Λ_1 's), transverselike (Λ_3 's), and purely transverse (Λ_2) branches, respectively, obtained by fitting the data to a three-nearest-neighbor Born–von Kármán model.

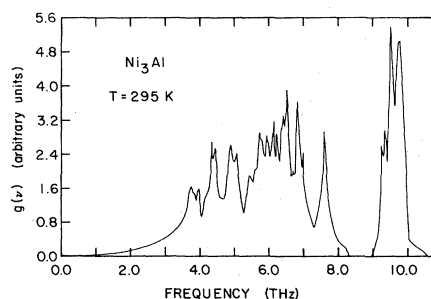


FIG. 4. Phonon density of states of Ni₃Al evaluated using the force constants listed in Table II.

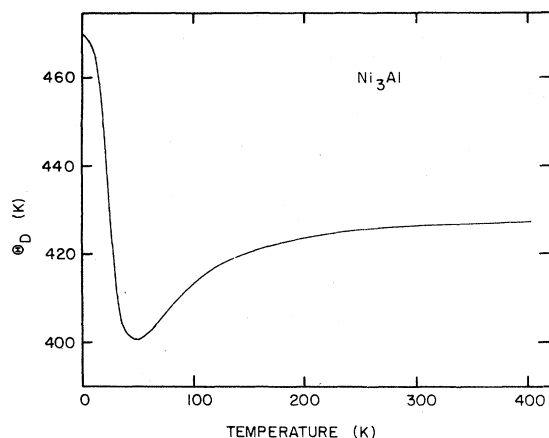


FIG. 5. Temperature dependence of the effective Debye temperature of Ni_3Al evaluated using the phonon density of states plotted in Fig. 4.

(plotted in Fig. 4) was used to calculate the lattice specific heat as a function of temperature and the results, expressed in terms of an effective Debye temperature Θ_D are plotted in Fig. 5. The Debye temperature at 0 K (470 K) obtained in the present analysis is in excellent agreement with the value (467 K) calculated from the measured elastic constants.¹⁴ These values, on the other hand, are considerably larger than those (330–390) obtained from the analysis of the low-temperature specific-heat measurements.^{4–6}

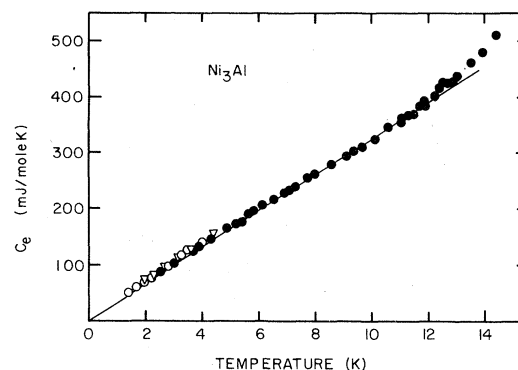


FIG. 6. Electronic specific heat of Ni_3Al obtained by subtracting the lattice contribution from measurements of total specific heat (\circ Ref. 4, ∇ Ref. 5, \bullet Ref. 6).

The electronic contribution to the total specific heat was obtained by subtracting the calculated lattice specific heat from the measured total specific heat of Ni_3Al (Fig. 6). It can be seen that the electronic specific heat does not exhibit any anomalous features at low temperatures. Thus, within the precision of the present analysis and of the specific-heat data, we do not find any evidence for the existence of magnetic inhomogeneities in Ni_3Al . The coefficient γ of the electronic specific heat obtained in the present analysis (32.7 mJ/mole K^2) is consistent with estimates obtained from specific-heat measurements,^{4–6} but it is approxi-

TABLE II. Room-temperature atomic force constants and elastic constants of Ni_3Al obtained by fitting the data to a three-nearest-neighbor Born–von Kármán model.

Atomic force constants	(10 ³ dynes/cm)	Elastic constants (10 ¹² dynes/cm ²)		
			Present work	Kayser and Stassis (Ref. 14)
Al-Ni 1XX	17.599	C_{11}	2.12	2.23
Al-Ni 1ZZ	-5.259	C_{44}	1.06	1.25
Al-Ni 1XY	1.535	C_{12}	1.25	1.47
Ni-Ni 1XX	18.180			
Ni-Ni 1ZZ	-0.936			
Ni-Ni 1XY	17.079			
Al-Al 2XX	-2.134			
Al-Al 2YY	-1.993			
Ni-Ni 2XX	6.737			
Ni-Ni 2YY	2.748			
Al-Ni 3XX	1.335			
Al-Ni 3YY	-0.658			
Al-Ni 3XZ	1.863			
Al-Ni 3YZ	8.235			
Ni-Ni 3XX	0.0105			
Ni-Ni 3YY	1.737			
Ni-Ni 3XZ	-0.378			
Ni-Ni 3YZ	0.589			

mately a factor of 2 larger than that evaluated^{10,11} from the electronic band structure of Ni₃Al. The origin of such a large discrepancy between the theoretical band calculations and the experimental values of the coefficient of the electronic specific heat is not clear at present. The discrepancy is too large to be accounted for by either the electron-phonon or electron-magnon²¹ enhancement of the electronic mass. It should be noticed, however, that the Stoner threshold of the magnetic excitations in Ni₃Al is expected to occur at relatively low energy, because of the small magnetic moment and low Curie temperature of this compound. As a result, the magnetic modes over most of the phase space are expected to behave more like paramagnons than magnons. The electron mass enhancement^{22,23} by these modes may thus be responsible for the observed large electronic specific

heat of Ni₃Al. Certainly a study of the magnetic excitations of Ni₃Al at low temperatures would help in understanding the origin of this large enhancement of the electronic specific heat. Such experiments are currently in preparation in this laboratory.

ACKNOWLEDGMENTS

The authors are grateful to Dr. S. H. Liu for many suggestions and to Dr. E. D. Halman for making available to us preliminary model calculations of the dispersion curves of Ni₃Al. Ames Laboratory is operated for the U. S. Department of Energy by Iowa State University under Contract No. W-7405-Eng-82. This research was supported by the Director for Energy Research, Office of Basic Energy Sciences, Grant No. WPAS-KC 02-02-01.

¹F. R. De Boer, C. J. Schinkel, and J. Biesterbos, *Phys. Lett.* **A25**, 606 (1967).

²F. R. De Boer, Ph.D. thesis, University of Amsterdam, 1969 (unpublished).

³F. R. De Boer, C. J. Schinkel, J. Biesterbos, and S. Proost, *J. Appl. Phys.* **40**, 1049 (1969).

⁴C. G. Robbins and H. Claus, *AIP Conf. Proc.* **5**, 527 (1971).

⁵R. W. Jones, G. S. Knapp, and C. W. Chu, *AIP Conf. Proc.* **10**, 1618 (1972).

⁶W. de Dood and P. F. de Chatel, *J. Phys. F* **3**, 1039 (1973).

⁷A. Parthasarathi and P. A. Beck, *AIP Conf. Proc.* **29**, 282 (1975).

⁸G. P. Felcher, J. S. Kouvel, and A. E. Miller, *Phys. Rev. B* **16**, 2124 (1977).

⁹T. F. M. Kortekass and J. J. M. Franse, *Phys. Status Solidi A* **40**, 479 (1977).

¹⁰G. C. Fletcher, *Physica (Utrecht)* **56**, 173 (1971); **62**, 41 (1972).

¹¹D. Hackenbracht and J. Kübler, *J. Phys. F* **10**, 427 (1980).

¹²R. W. Coward and J. H. Westbrook, *Trans. Metall.*

Soc. AIME **215**, 807 (1959).

¹³P. A. Flinn, *Trans. Mater. Sci.* **10**, 151 (1963).

¹⁴F. X. Kayser and C. Stassis, *Phys. Status Solidi A* **64**, 335 (1981).

¹⁵T. L. Johnston, A. S. Tetelman, and A. J. McEvily, Jr., *Proceedings of the Second International Materials Conference*, Berkeley, California, June, 1964, edited by V. F. Zackey (Wiley, New York, 1965).

¹⁶R. G. Davies and N. S. Stoloff, *Trans. Metall. Soc. AIME* **233**, 714 (1965).

¹⁷J. de Klerk, *Proc. Phys. Soc. (London)* **73**, 337 (1959).

¹⁸R. J. Birgeneau, J. Cordes, G. Colling, and A. D. B. Woods, *Phys. Rev.* **136**, A1359 (1964).

¹⁹G. A. Dewit and B. N. Brockhouse, *J. Appl. Phys.* **39**, 451 (1968).

²⁰This technique is essentially an extension of the interpolation method of G. Gilat and L. J. Raubenheimer, *Phys. Rev.* **144**, 390 (1966).

²¹L. C. Davis and S. H. Liu, *Phys. Rev.* **163**, 503 (1967).

²²N. F. Berk and J. R. Schrieffer, *Phys. Rev. Lett.* **17**, 433 (1966).

²³S. Doniach and S. Engelsberg, *Phys. Rev. Lett.* **17**, 750 (1966).